International Journal of Impact Engineering 38 (2011) 85–94

Contents lists available at ScienceDirect

International Journal of Impact Engineering

journal homepage: www.elsevier.com/locate/ijimpeng

Dynamic bending response of double cylindrical tubes filled with aluminum foam

Liuwei Guo, Jilin Yu*

CAS Key Laboratory of Mechanical Behavior and Design of Materials, University of Science and Technology of China, Hefei, Anhui 230027, People's Republic of China

ARTICLE INFO

Article history:
Received 6 April 2010
Received in revised form
3 October 2010
Accepted 4 October 2010
Available online 12 October 2010

Keywords:
Foam-filled structure
Double tube structure
Aluminum foams
Dynamic bending behavior
Crashworthiness

ABSTRACT

The dynamic three-point bending behavior of double cylindrical tubes filled with closed-cell aluminum foam core was studied experimentally and numerically. It is found that the deformation mode of this new structure under impact loading is different to that under quasi-static loading. The load carrying capacity of the structure subjected to impact remains at the level of that in the quasi-static situation. Compared with traditional foam-filled single tubes, the specific energy absorption efficiency of this new structure is much higher, and that of both foam-filled structures in the dynamic situation are higher than that in static situation. A preliminary experimental study on the effect of profiles and span of the structure were performed, and the result shows that these parameters affect the structure together. Numerical simulation of the bending behavior was also executed with the explicit finite element method. The mechanism of the dynamic response is revealed by comparison of the maximum strain history in the simulation.

1. Introduction

During the past two decades, much research work on the axial crushing behavior of thin-walled columns has been carried out to find more effective energy absorbers [1–3]. On the other hand, a study on the real world vehicle crashes presented by Kallina et al. [4] in 1994 showed that up to 90% involved structural members failed in bending collapse mode.

The bending resistance of an empty thin-walled column typically declines very significantly after reaching the peak force at a small rotation. In order to achieve high bending resistance and weight efficiency in energy absorption, ultra-light cellular metals such as aluminum foams were introduced to fill in thin-walled empty structures. The bending behaviors of such structures have been studied by many researchers. Santosa and Wierzbicki [5] and Santosa et al. [6] studied the effect of foam filling on the bending resistance of thin-walled prismatic columns through numerical simulations and quasi-static experiments. Their result shows that the filling of foam improves the load carrying capacity by offering additional support from inside and increases the energy absorption. Chen et al. [7] performed optimization for minimum weight on foam-filled sections under bending condition. They showed the potential of thin-walled columns filled with aluminum foams as weight-efficient energy absorbers. Chen [8] studied the bending behavior of hat profiles filled with aluminum foams and found that filling of aluminum foams increased the specific energy absorption of the structures. Kim et al. [9] studied the bending collapse of thin-walled cylindrical tubes filled with several pieces of foams experimentally and numerically. Hanssen et al. [10] studied the bending behavior of the foam-filled square extrusions experimentally and found that the foam filler altered the local deformation patterns of the beams significantly. Reyes et al. [11] presented numerical analyses of foam-filled extrusions subject to bending. They found that taking fracture in both the extrusion and the foam into account in the analyses was very important, and the predicted behavior depended on the choice of fracture criterion and its critical value used for the foam, the statistical variation of foam density.

Most studies in the literature focused on the prismatic column structures and mainly under quasi-static loading. In order to improve the crashworthiness of foam-filled structures while keeping high bending resistance under impact condition, the dynamic bending behavior of a new composite structure, i.e. double cylindrical tubes filled with closed-cell aluminum foams, is studied in detail in this paper. Dynamic experiments and finite element simulations are performed to explore the deformation and failure mechanism of the structure. The results are compared with those under quasi-static loading [12] and those of empty and foam-filled single tubes.

2. Experimental procedures

2.1. Materials and specimens

Three types of tube structures, i.e., empty tube, foam-filled single tube and foam-filled double tube, were used in the

* Corresponding author. Tel.: +86 551 360 0792; fax: +86 551 360 6459.
E-mail address: jlyu@ustc.edu.cn (J. Yu).

0734-743X/$ – see front matter © 2010 Elsevier Ltd. All rights reserved.
doi:10.1016/j.ijimpeng.2010.10.004

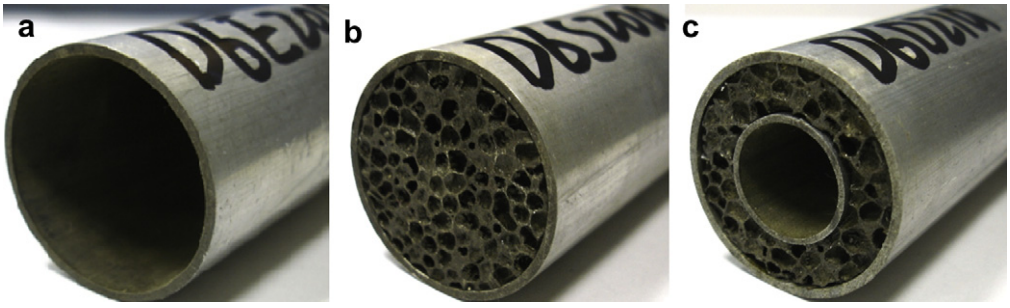

Fig. 1. The sections of (a) empty tube, (b) foam-filled single tube and (c) foam-filled double tube.

experiments. The cross-sections of different tube structures are shown in Fig. 1. The tube material used in our experiments is AA6063-T6 aluminum. The uniaxial tension test of tube material with three kinds of thicknesses, i.e. 1.0, 1.6 and 2.0 mm, was carried out. The engineering stress–strain curves have slight differences as shown in Fig. 2, which may be caused by the different extrusion ratio of the profiles. The closed-cell aluminum foam was provided by Luoyang Ship Material Institute, CSIC, China and produced by liquid state processing using TiH_2 as foaming agent. The uniaxial quasi-static compression test results of the foams are shown in Fig. 3 where ρ_f denotes the apparent density of the foam.

Table 1 gives the dimensions of the cylindrical tubes in the experiments. The parameters of specimens are listed in Table 2. In this paper, specimens are named according to the following rule. The first letter in the specimen named "D6D21a" means the experiment is under dynamic loading condition, and for the static test, the first letter does not exist, e.g. "6D21a". The number following the first letter denotes the ratio of the span L_0 to the diameter D of the outer tube. The third letter means the arrangement or filling status that E means empty tube, S means foam-filled single tube and D means foam-filled double tube structure. The fourth and fifth number means the types of the outer tube and inner tube respectively, detailed dimensions of which are listed in Table 1. The last letter is the serial number of test.

2.2. Arrangement of experiments

The dynamic three-point bending tests as illustrated in Fig. 4 were conducted on a drop weight machine. The mass of the hammer was 24.23 kg and the drop height was 141.8 cm. The initial impact energy is about 336 J, which is enough to destroy the specimens in the experiments. The diameter of the cylindrical punch and supports is 10 mm. The angle between two wedged sides of the upper punch is 34.6 degree. The span length L_0 of different arrangements depends on the ratio L_0/D and the diameter D of outer profiles. The total length of the structure L_1 is 190 mm when L_0/D is 4, and 270 mm when L_0/D is 6. Two rubber bands were used on the two sides of the specimen to avoid jump of the specimen on the vertical direction.

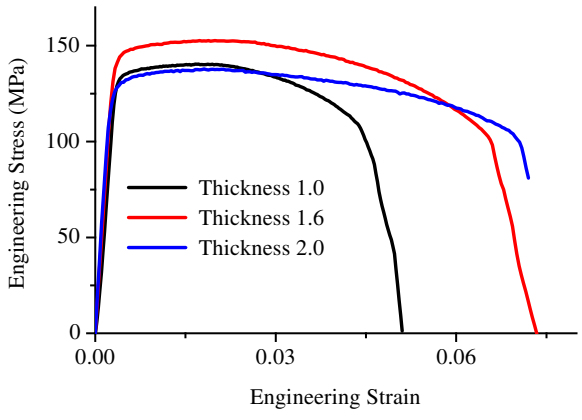

Fig. 2. The uniaxial tensile stress–strain curves of profile material.

2.3. Definitions

The total energy absorbed by a structure before failure is calculated by

$$E_t = \int_0^{U_f} F\mathrm{d}u,$$

where F is the bending force, u the displacement of the upper punch, and U_f the displacement of the upper punch at failure of the structure, when the force sharply falls down. The mass efficiency of the energy absorption for a structure is defined by

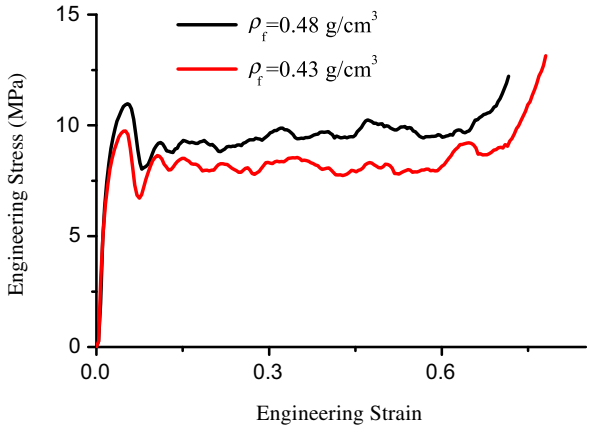

Fig. 3. The uniaxial compression stress–strain curves of aluminum foams.

Table 1
Dimensions of outer and inner cylindrical tubes.

	Outer profiles		Inner profiles	
	Diameter (mm)	Thickness (mm)	Diameter (mm)	Thickness (mm)
1	38	1.0	20	1.2
2	38	1.6	24	1.2
3	38	2.0	22	1.4

Table 2
Measured parameters of specimens.

Specimen	Profiles (outer tube/inner tube)		Aluminum foam		m_t (g)	U_f (mm)	E_t (J)	E_s (J/g)
	Thickness (mm)	Mass (g)	Mass (g)	Density (g/cm^3)				
D4E20a	1.6/0	124.6/0	–	–	124.6	–	–	–
D4E20b	1.6/0	124.5/0	–	–	124.5	–	–	–
D4E20c	1.6/0	124.4/0	–	–	124.4	–	–	–
D4S20a	1.6/0	124.3/0	118.2	0.46	170.6	23.2	151.8	0.89
D4S20b	1.6/0	124.4/0	97.7	0.38	156.3	22.6	117.4	0.75
D4S20c	1.6/0	124.4/0	120.4	0.47	172.3	21.8	141.8	0.82
D4D21a	1.6/1.2	124.6/42.4	69.6	0.40	166.5	52.7	333.6	2.00
D4D21b	1.6/1.2	124.2/42.3	75.1	0.44	170.0	50.5	304.4	1.79
D4D21c	1.6/1.2	124.4/42.4	70.5	0.41	167.0	56.9	331.2	1.98
D6E20a	1.6/0	124.5/0	–	–	124.5	–	–	–
D6E20b	1.6/0	124.5/0	–	–	124.5	–	–	–
D6E20c	1.6/0	124.4/0	–	–	124.4	–	–	–
D6S20a	1.6/0	124.5/0	103.1	0.40	227.6	21.2	91.5	0.40
D6S20b	1.6/0	124.5/0	121.4	0.47	245.9	17.4	80.5	0.33
D6S20c	1.6/0	125.5/0	119.0	0.46	243.5	18.8	85.2	0.35
D6D21a	1.6/1.2	124.5/42.4	82.3	0.48	249.2	43.2	190.5	0.76
D6D21b	1.6/1.2	124.5/42.4	77.1	0.45	244.0	47.1	205.5	0.84
D6D21c	1.6/1.2	124.5/42.4	71.3	0.41	238.2	45.5	186.0	0.78
D6D11a	1.0/1.2	83.6/42.4	98.4	0.52	224.4	29.9	104.6	0.47
D6D11b	1.0/1.2	83.6/42.4	96.1	0.51	222.1	33.3	115.0	0.52
D6D11c	1.0/1.2	83.6/42.4	96.9	0.51	222.9	27.6	109.4	0.49
D6D31a	2.0/1.2	153.4/42.4	85.4	0.53	281.2	56.5	298.6	1.10
D6D31b	2.0/1.2	153.4/42.4	83.7	0.52	279.5	61.5	306.7	1.10
D6D31c	2.0/1.2	153.4/42.4	86.5	0.54	282.3	50.0	242.5	0.88
D6D22a	1.6/1.2	124.8/51.4	61.1	0.45	237.3	69.6	286.3	1.20
D6D22b	1.6/1.2	124.8/51.4	71.0	0.53	247.2	75.0	290.4	1.17
D6D22c	1.6/1.2	124.8/51.4	64.0	0.48	240.2	83.9	300.6	1.25
D6D23a	1.6/1.4	124.7/59.5	75.7	0.49	259.9	50.0	256.5	0.99
D6D23b	1.6/1.4	124.7/59.5	75.6	0.49	259.8	48.3	239.0	0.92
D6D23c	1.6/1.4	124.7/59.5	77.0	0.50	261.2	42.3	226.7	0.87

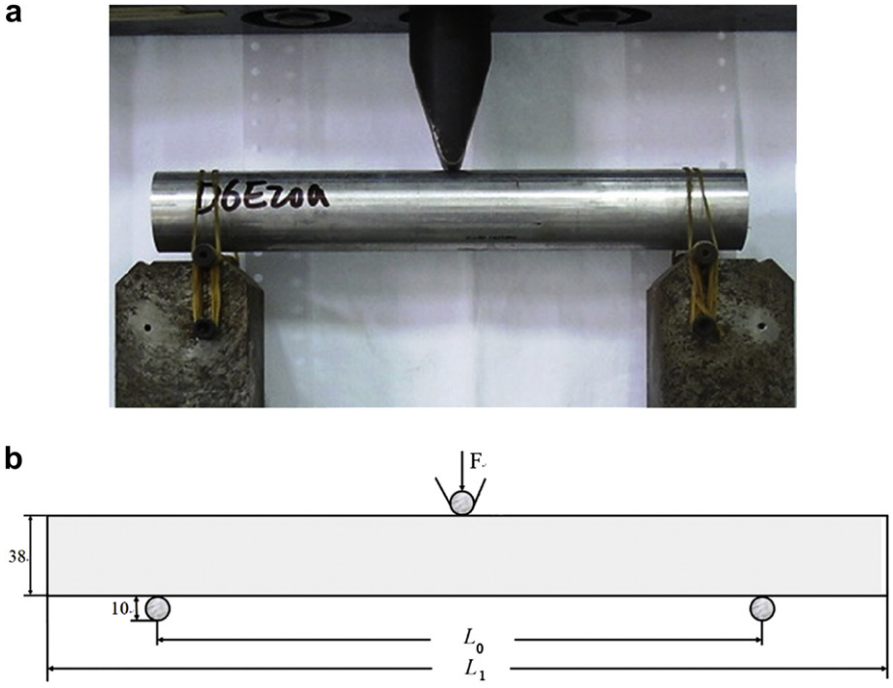

Fig. 4. (a) Setup and (b) the model of the dynamic three-point bending tests.

$$E_s = E_t/m_t,$$

where m_t is the total mass of the structure.

2.4. Reproducibility of experiments

In the experiments, three samples of each structure were executed. The reproducibility for each type of structure is shown in Fig. 5. There are more or less differences for each type of specimens, which may be caused by the scatter of the foam density and different imperfections of each specimen. In order to make the comparisons for different structures easier, only one curve of each structure will be chosen and used in comparisons thereafter.

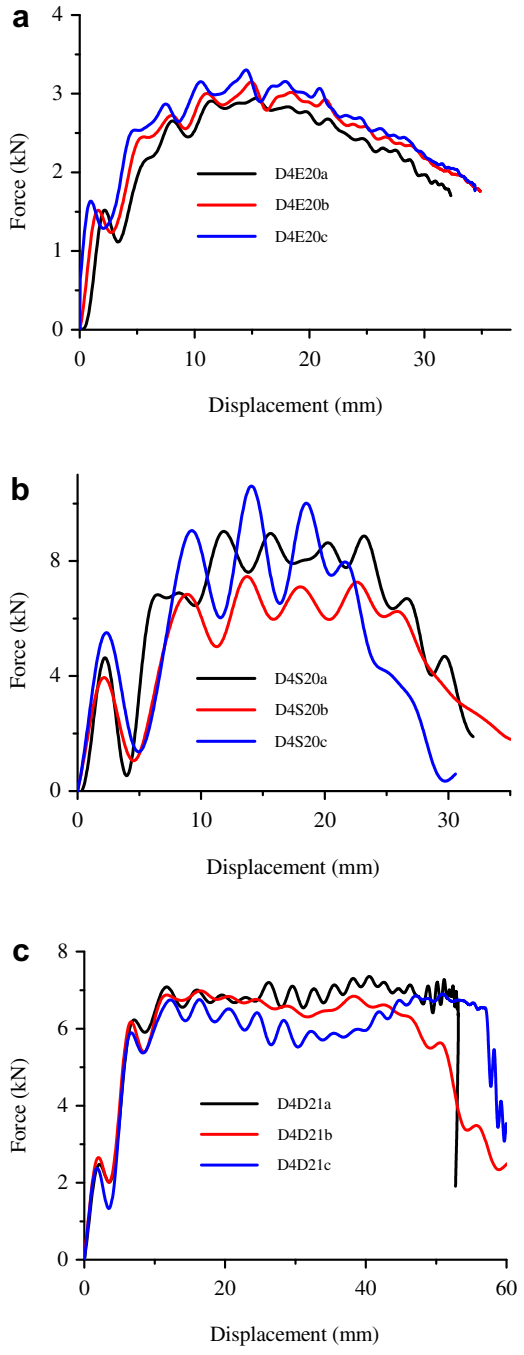

Fig. 5. The reproducibility of bending tests of (a) empty tubes, (b) foam-filled single tubes and (c) foam-filled double tubes.

3. Experimental results and discussion

3.1. Deformation and failure mode

Typical deformation and failure of foam-filled structures after impact are shown in Fig. 6. The crack of the foam-filled single tube occurs almost underneath the hammer but that of the foam-filled double tube is located at one side of the hammer, which consists with the observation in quasi-static tests [10]. It was also observed that the foam-filled single tube ruptured completely but the inner tube of the foam-filled double tube structure was still undamaged while the structure ruptures.

A comparison of the failure mode of the foam-filled double tubes under static and dynamic loads is shown in Fig. 7. Two cracks are found on the outer profile in the quasi-static test, but only one leads to the final failure of the structure. On the other side, the situation is not so obvious in the dynamic case. Under impact conditions, the outer profile of the foam-filled double tube ruptures at one side from the center, but there are more than two cracks inside the foam, spreading widely along the down part in the center region, which may lead to an increase in energy absorption. The difference in failure mode between the static and dynamic cases will be discussed later in detail in the section on numerical simulation.

3.2. Load carrying capacity and energy absorption

Comparisons of the force–displacement curves of different structures with two values of span under impact bending condition are shown in Fig. 8. For both spans, the load carrying capacity of the empty tube declines seriously but that of foam-filled double tube structure is much steadier, especially with $L_0/D = 4$. Compared with that of the traditional foam-filled single tube, the force of the foam-filled double tube with $L_0/D = 4$ is lower but almost the same level of force is found for both structures with $L_0/D = 6$. The foam-filled double tube fails much later and its failure displacement U_f is about twice as that of the foam-filled single tube, indicating that more impact energy can be absorbed. It can also be observed that the curves of foam-filled structures with $L_0/D = 6$ oscillate more seriously than that with $L_0/D = 4$. But the force oscillation of the foam-filled double tube with $L_0/D = 6$ decreases rapidly as the displacement increases.

The force–displacement curves of the foam-filled structures under impact bending are also compared with those in quasi-static cases, as plotted in Fig. 9. It shows that the load carrying capacity of the foam-filled structures in dynamic cases is almost at the same level as that in the corresponding quasi-static cases, or even slightly higher for some structures. However, the failure displacement, U_f, subjected to an impact load is larger than that subjected to a quasi-static load for all foam-filled single and double tubes. As the deformation mode reveals, more energy under the impact condition may be absorbed by the upper part of the structure and the foam inside, so less energy was dissipated on the lower profiles, which leads to the delayed failure of foam-filled structures under the impact condition. And the direct mechanism may be the slightly delayed strain evolution of the lower outer profile under dynamic loading, which will be proved in the numerical simulation later.

Comparisons of the energy absorption of different structures under quasi-static and dynamic loading are shown in Fig. 10. Results of the empty tubes are not included because their force drops rapidly without obvious failure point. It should be mentioned

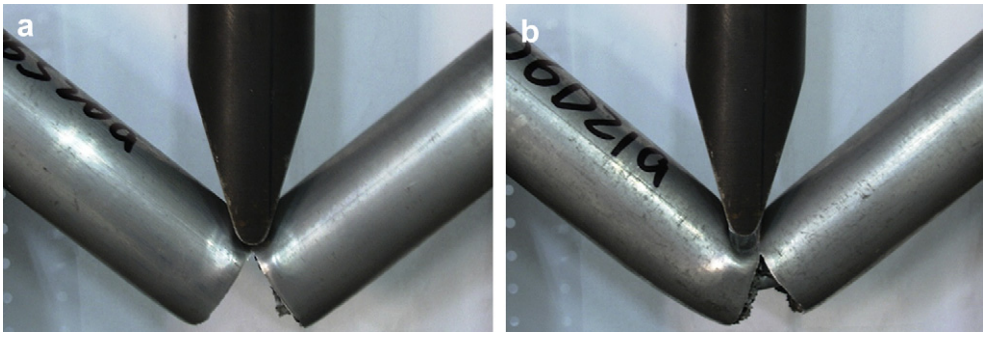

Fig. 6. The dynamic deformation and failure of (a) foam-filled single tube D6S20a and (b) foam-filled double tube D6D21a.

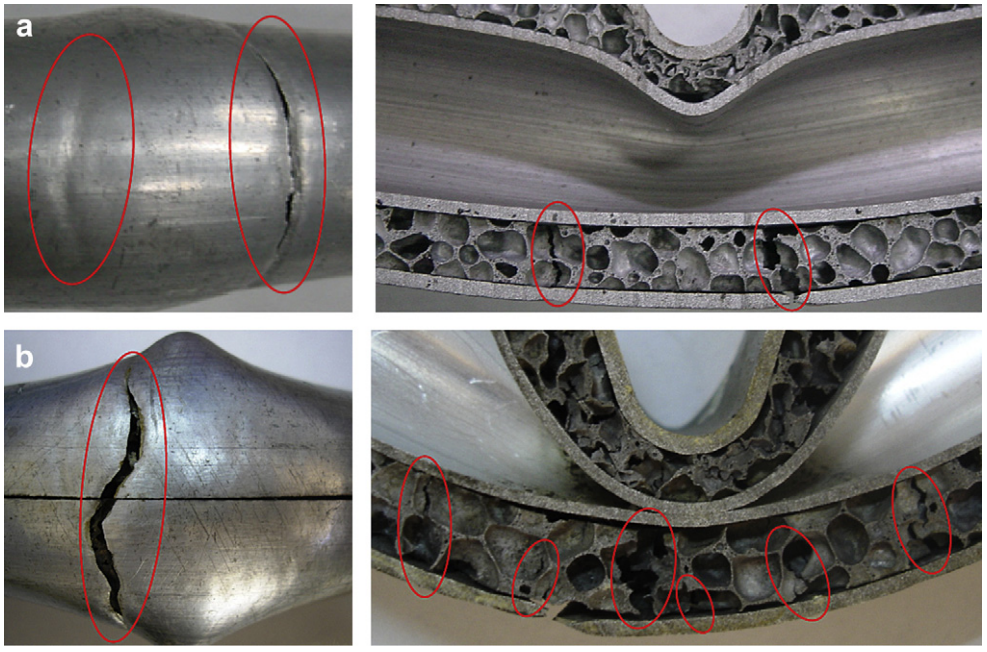

Fig. 7. Comparisons of the deformation and failure of foam-filled double tube D6D21c in (a) quasi-static [12] and (b) dynamic tests.

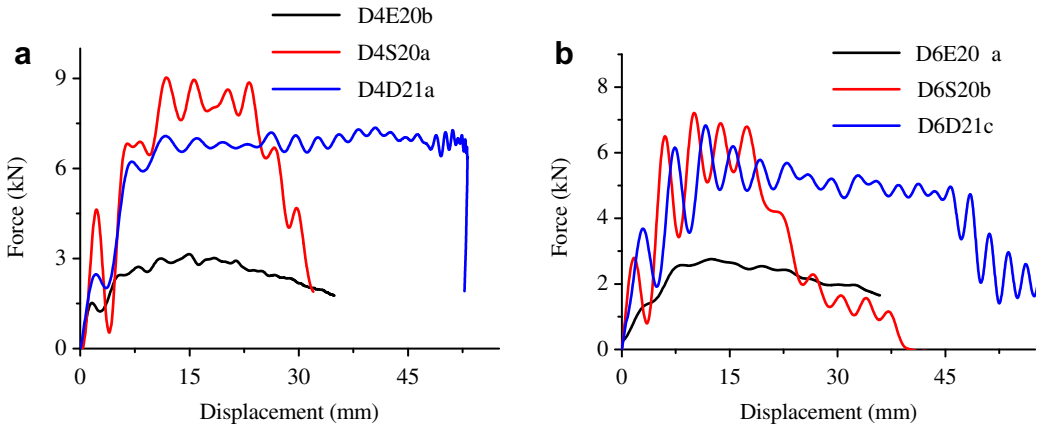

Fig. 8. Comparisons of the force–displacement curves of different structures with different spans under impact condition: (a) $L_0/D = 4$ and (b) $L_0/D = 6$.

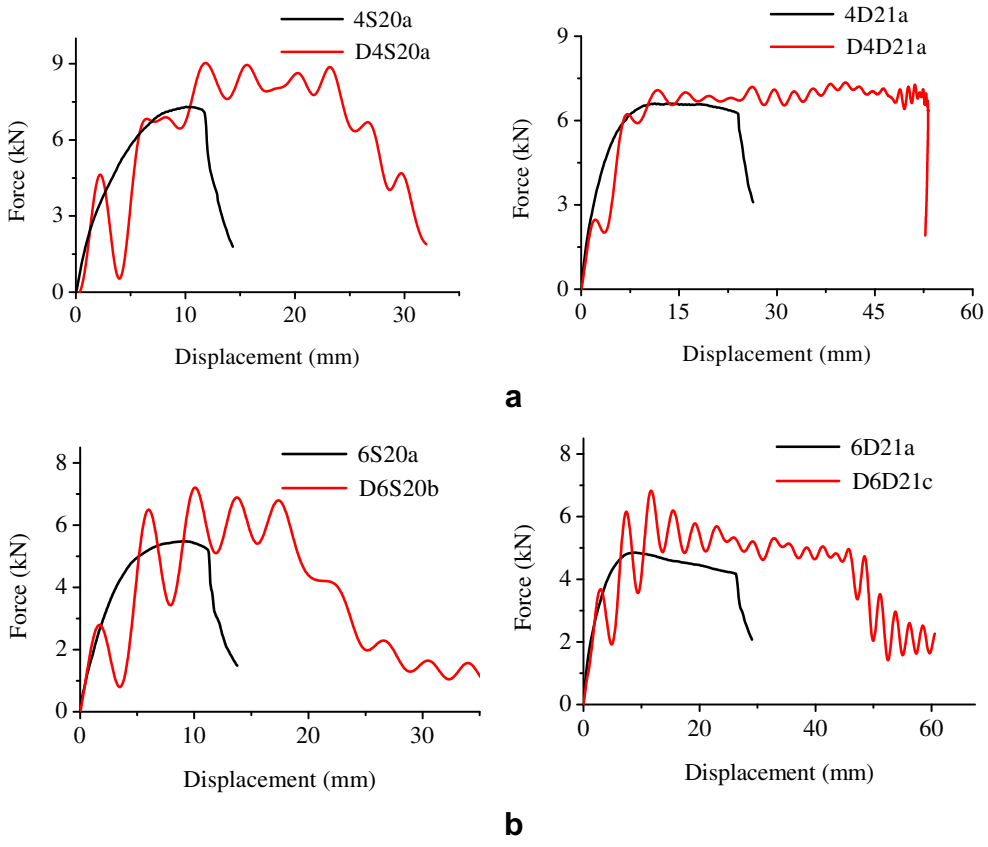

Fig. 9. Comparisons of the force–displacement curves of foam-filled structures under quasi-static and dynamic loads: (a) $L_0/D = 4$ and (b) $L_0/D = 6$.

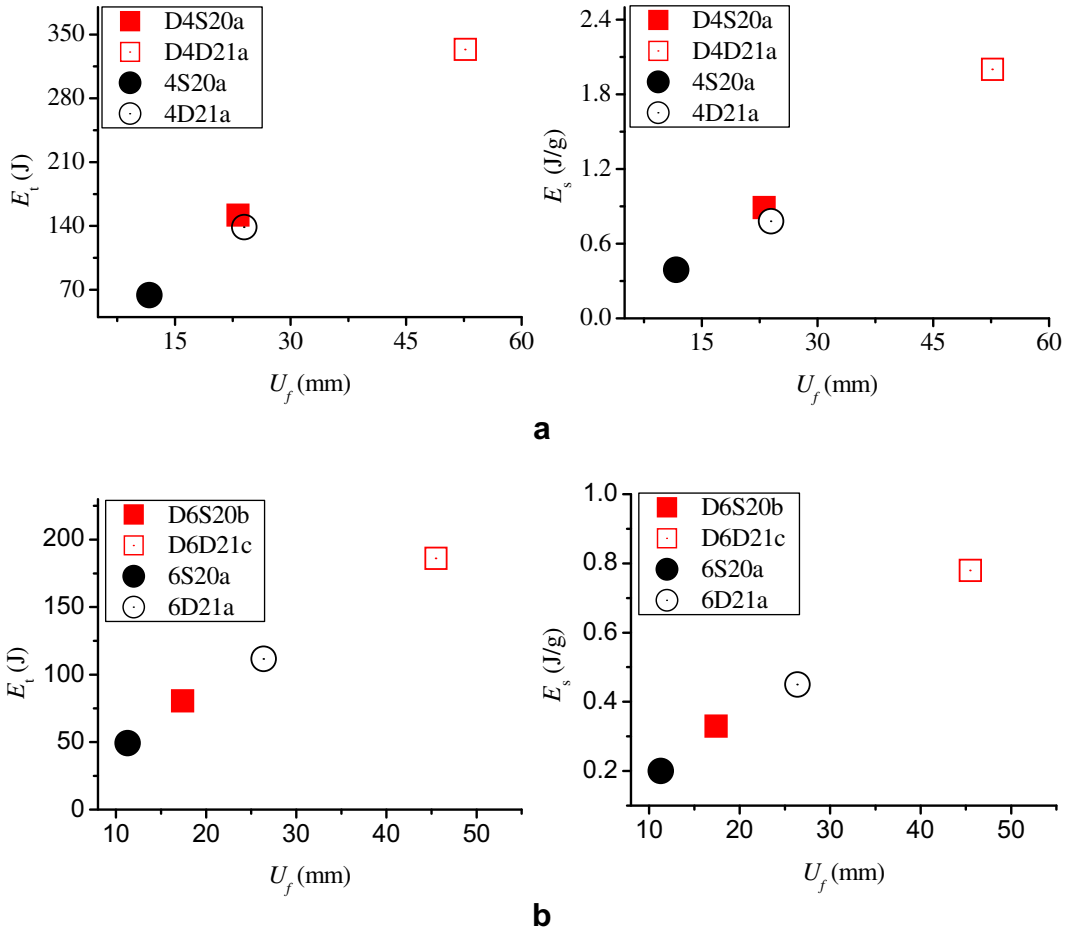

Fig. 10. Comparisons of the energy absorption of foam-filled structures under quasi-static and dynamic loads: (a) $L_0/D = 4$ and (b) $L_0/D = 6$.

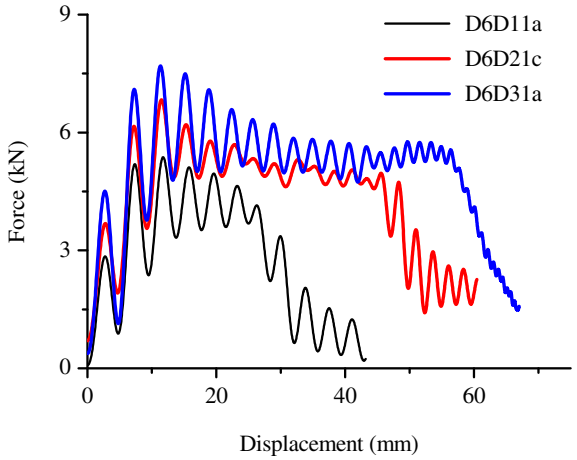

Fig. 11. Comparisons of the force–displacement curves of foam-filled double tube with different outer tube thicknesses under impact condition.

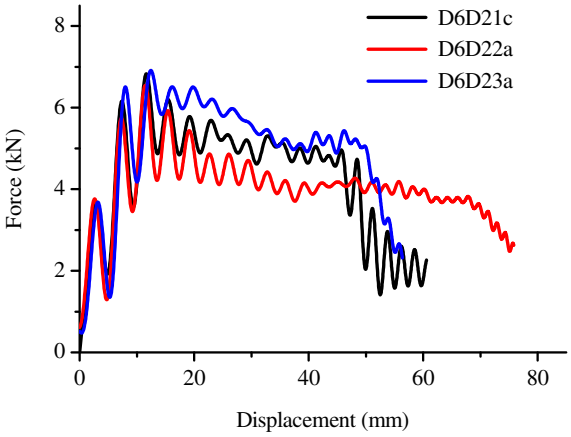

Fig. 13. Comparisons of the force–displacement curves of foam-filled double tubes with different inner tubes under impact condition.

that the mass of the foam-filled double tube is almost the same as the traditional foam-filled single tube, as shown in Table 2. With both spans, the total energy absorption and the mass efficiency of the foam-filled double tubes are much higher than those of the traditional foam-filled single tubes, no matter in quasi-static cases or under the impact condition. And the energy absorption of all the foam-filled structures in dynamic tests is higher than that in the corresponding quasi-static ones. The total energy absorption and the mass efficiency of the foam-filled double tube in dynamic cases are about twice of the foam-filled single tube with $L_0/D = 4$ and nearly thrice for $L_0/D = 6$. The advantage in energy absorption for the foam-filled double tube structure comes from the larger failure displacement due to the special geometry.

3.3. Effect of outer tube thickness

Three kinds of outer tubes in different thicknesses, as shown in Table 1, were tested to study the effect of the outer tube thickness on the impact responses of foam-filled double tube structures. The force–displacement curves are plotted in Fig. 11. It shows that thickening the outer tube increases both the load carrying capacity and the failure displacement, U_f, and the oscillation of the force remains at the same level.

The effect of the outer tube thickness on the energy absorption capacity of the foam-filled double tube was also studied and the results are shown in Fig. 12. It can be found that thickening the outer tube increases the total and specific energy absorption of the structure, in the parameter range of current experiments.

3.4. Effect of the inner tube

Three types of inner tubes shown in Table 1 were used in the impact tests to investigate the effect of the inner tube diameter and thickness on the impact responses of foam-filled double tube structures. The force–displacement curves are plotted in Fig. 13. With the increase of the inner tube diameter, the load carrying capacity decreases but the failure displacement becomes larger and the oscillation of the force becomes smaller. Thickening the inner tube increases the load carrying capacity but reduces the failure displacement.

Within the current experiment range, enlarging the inner tube increases the total energy absorption, as well as the mass efficiency of the structure, as shown in Fig. 14. Thickening the inner tube is not as effective as enlarging the inner tube in increasing the mass efficiency of the energy absorption. Nevertheless, the detailed effect of the inner tube is needed to be studied in the future since

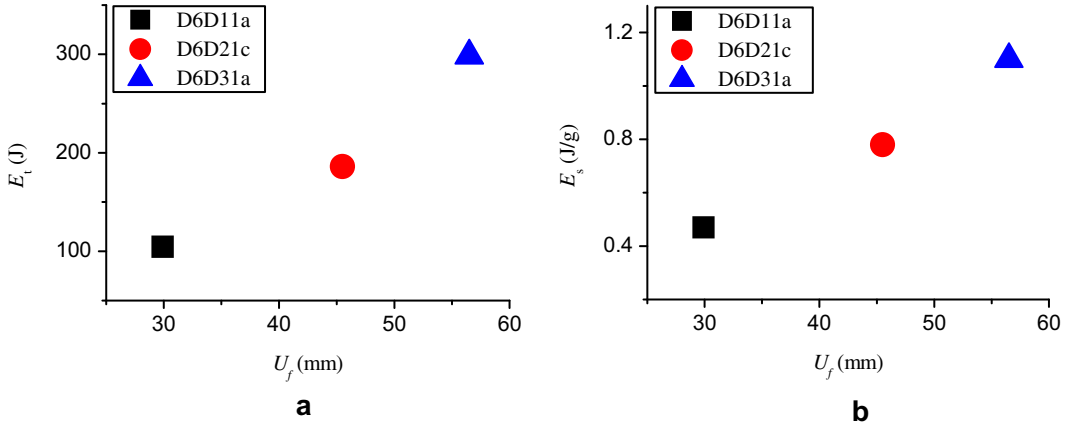

Fig. 12. Comparisons of the energy absorption of foam-filled double tubes with different outer tube thicknesses under impact condition: (a) total energy absorption and (b) specific energy absorption.

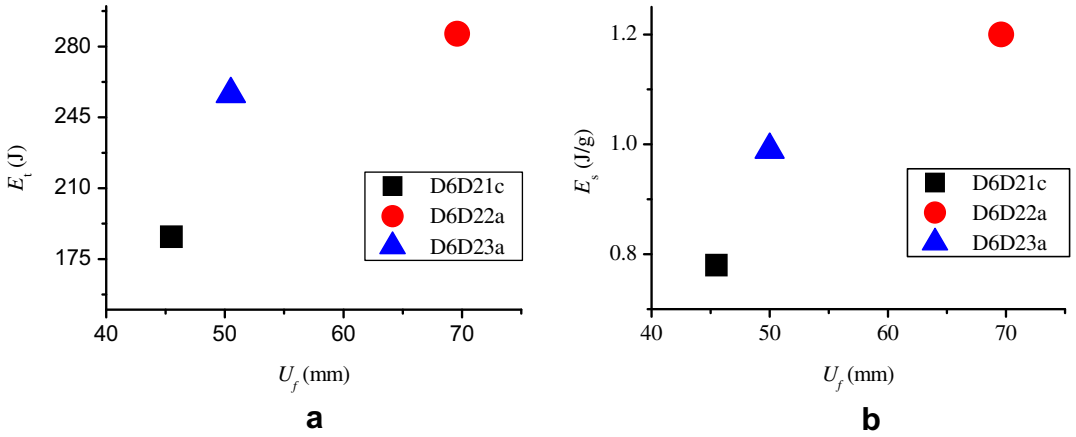

Fig. 14. Comparisons of the energy absorption of foam-filled double tubes with different inner tubes under impact condition (a) total energy absorption (b) specific energy absorption.

only limited inner tube types were studied in the present experimental investigation.

4. Numerical simulation

In order to explore the mechanism of deformation and failure, numerical simulation of the foam-filled double tube structure D6D21, as well as the foam-filled single tube D6S20, were conducted using the explicit finite element code ABAQUS. The material parameters used in the simulation were obtained from the experiments [12]. The elastic-plastic model with isotropic strain hardening and associated flow rule was used for the profiles. The engineering stress–strain curves obtained from the experimental results have been transformed to the true stress-plastic strain curves. The crushable foam model developed originally by Deshpande and Fleck (2000) are used for the aluminum foam core. The detailed material parameters are shown in Table 3. The impact velocity and boundary conditions are all the same as those in experiments.

Table 3
The material parameters in detail.

	ρ (g/cm^3)	E (GPa)	ν	ν_p	k
Tube	2.7	59	0.3		
Foam	0.43	0.625	0.1	0	1.732

As shown in Fig. 15, the dynamic simulation results are in good agreement with the experimental results. Since no failure criterion of the foam and tube material was considered in this simulation, the results differ from the experimental results at the late stage when the structure starts to fracture in the experiment.

In order to understand the deformation and failure mechanism of the foam-filled structures subjected to impact loading, the maximum equivalent plastic strain ε_m at the lower part of the outer profile near the center is checked in the simulation. The curves of the maximum equivalent plastic strain ε_m to the displacement U_u of the upper punch for foam-filled structures are shown in Fig. 16. With the increase of the upper punch displacement, the maximum strain ε_m of the foam-filled single tube increases much more rapidly than the foam-filled double tube. In other words, having the same equivalent plastic strain in the lower part of the outer profile, the deflection of the foam-filled double tube structure is much larger than the traditional foam-filled single tube. So, it could absorb much more energy than the traditional foam-filled single tube.

As the experiments reveal, the failure displacement U_f of foam-filled tube structures under dynamic loading is larger than that under quasi-static loading. In order to understand the mechanism, the maximum equivalent plastic strains ε_m of the foam-filled

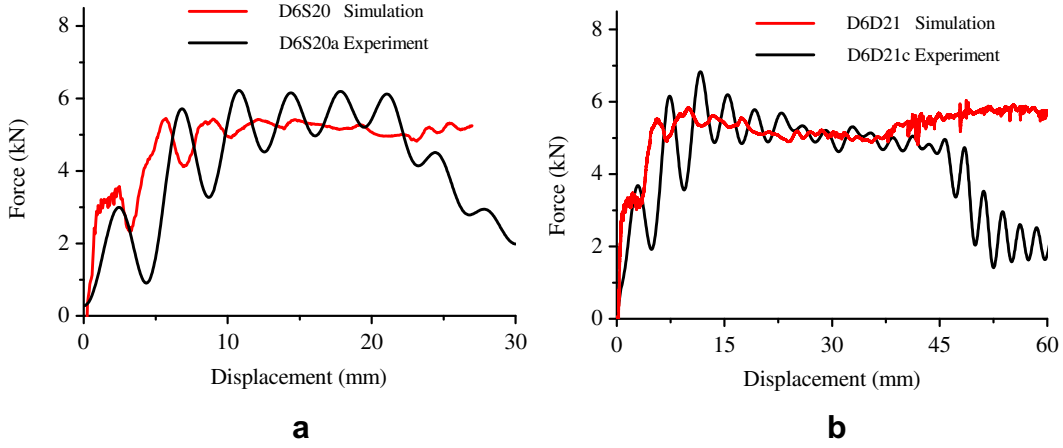

Fig. 15. Comparisons of experimental and numerical results of force–displacement curves of (a) foam-filled single tube and (b) foam-filled double tube.

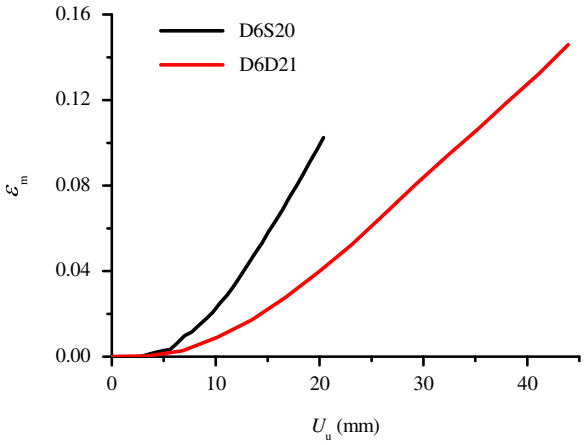

Fig. 16. The $\varepsilon_m - U_u$ curves of foam-filled structures under impact condition.

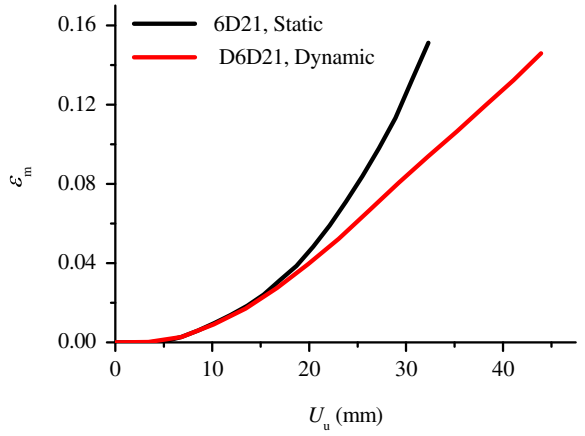

Fig. 17. A comparison of the static and dynamic $\varepsilon_m - U_u$ curves for foam-filled double tubes.

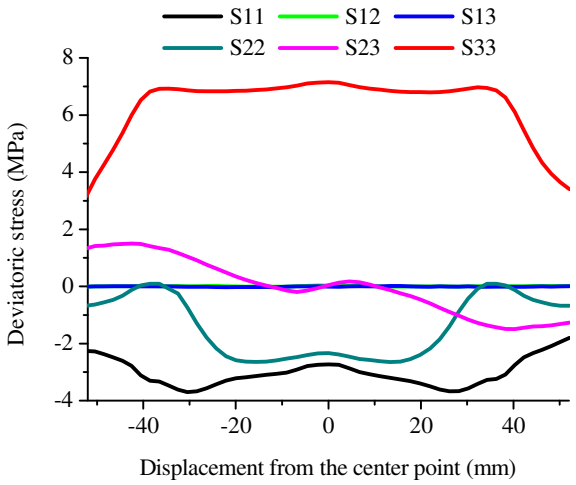

Fig. 19. The deviatoric stress distributions along the lower line of the foam in the foam-filled double tube D6D21.

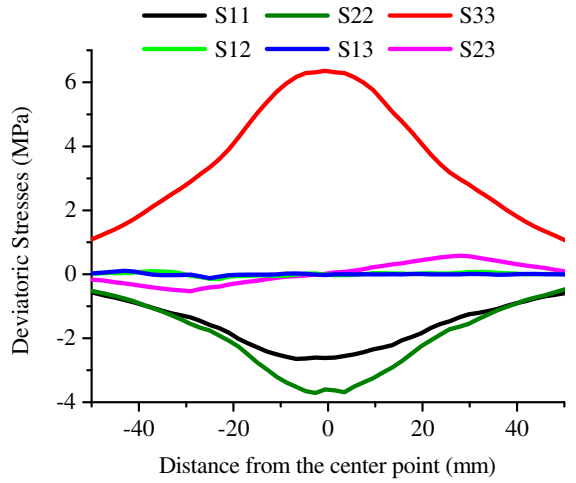

Fig. 20. The deviatoric stress distributions along the lower line of the foam in a foam-filled single tube.

double tube D6D21 under static and dynamic loading conditions are compared in Fig. 17. It shows that the maximum strain ε_m in dynamic case increases slower than that in static case, which may be a reason for the failure displacement in dynamic case being larger than that in static case (Fig. 1) (Fig. 19).

The deformation of the foam in the foam-filled double tube structure is shown in Fig. 18. In order to investigate the failure mechanism of the foam under impact loading, the deviatoric stresses of the foam with the span $L_0/D = 6$ were studied in the simulation and their distributions along the lower line of Fig. 18 are shown in Fig. 19. The deviatoric tensile stress in the axial direction, s_{33}, is high and almost constant in a wide region (about 70 mm) near the center, which differs from the quasi-static case where two peaks occur in both sides. This may be a possible explanation for the spread multi-cracks in the foam found in the experiments. For comparison, the distribution of deviatoric stresses in a foam-filled single tube is shown in Fig. 20, which explains the difference in failure mode between the two kinds of structure (Fig. 3).

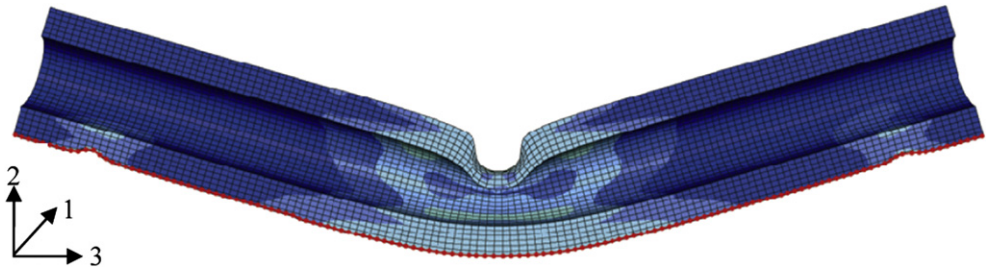

Fig. 18. The deformation of the foam inside the foam-filled double tube D6D21.

5. Conclusions

Dynamic bending responses of foam-filled double tube structures were studied experimentally and numerically in this paper. In comparison with the traditional foam-filled single tube, this new structure has a steadier load carrying capacity and much higher energy absorption efficiency, which is a great potential as an energy absorber under bending conditions. The effect of profiles and the span on the dynamic responses for this structure was also investigated in the experiments. Results show that they affect the structural response in conjunction with each other. With proper parameters, a steady load carrying capacity and high-energy absorption efficiency can be achieved.

Under the impact condition, the maximum equivalent plastic strain increases with the displacement of the upper punch of this new structure much slower than that of the foam-filled single tube, as found in the simulation. This increases its ability of energy absorption. In comparison with the quasi-static case, the maximum equivalent plastic strain of the foam-filled tube structures under dynamic condition increases slower, which gives a reason for the difference of the displacement before failure between the quasi-static and dynamic results.

Experiments show that failure of the foam-filled double tube structure under impact loading results from multiple cracks spreading in the foam, followed by outer profile failure, which differs from the quasi-static case where only two cracks were found in the foam. As pointed by Reyes et al. [11], taking fracture in both the profile and the foam into account in the numerical analyses was very important. However, a reliable or well accepted failure criterion of aluminum foam has not been identified yet, especially for the case of multi-axial deformation. Hence we did not take any failure criterion in the numerical simulation, and the results are not suitable for the later response and can not be used to predict the failure of the structure. Nevertheless, a nearly constant deviatoric stress distribution in the axial direction of the foam is found in numerical simulation, which may explain the finding of multi-cracks in the foam, and high-energy absorption capacity of the foam-filled double tube found in the impact tests. Of course, further study on the failure criteria should be done both experimentally and numerically.

Restricted to the types of tubes, the effects of the parameters on the energy absorption property of the new structure have not been fully explored in current experiments. More detailed experiments need to be conducted in the near future.

Acknowledgements

The results reported in this paper were supported by the National Natural Science Foundation of China (projects numbers 90916026, 10672156, 10532020 and 90205003).

References

[1] Wierzbicki T, Abramowicz W. On the crushing mechanics of thin-walled structures. Journal of Applied Mechanics 1983;50:727–39.
[2] Abramowicz W, Wierzbicki T. Axial crushing of foam-filled columns. International Journal of Mechanical Sciences 1988;30(314):263–71.
[3] Seitzberger M, Rammerstorfer F, Gradinger R, Degischer H, Blaimschein M, Walch C. Experimental studies on the quasi-static axial crushing of steel columns filled with aluminum foam. International Journal of Solids and Structures 2000;37:4125–47.
[4] Kallina I, Zeidler F, Baumann K, Scheunest D. The offset crash against a deformable barrier, a more realistic frontal impact. In: Proceedings of the 14th International Technical Conference on Enhanced Safety of Vehicles, vol. 2. Washington, DC: National Highway Traffic Safety Administration; 1994. p. 1300–4.
[5] Santosa S, Wierzbicki T. Effect of an ultralight metal filler on the bending collapse behavior of thin-walled prismatic columns. International Journal of Mechanical Sciences 1999;41:995–1019.
[6] Santosa S, Banhart J, Wierzbicki J. Experimental and numerical analyses of bending of foam-filled sections. Acta Mechanica 2001;148:199–213.
[7] Chen W, Wierzbicki T, Santosa S. Bending collapse of thin-walled beams with ultralight filler: numerical simulation and weight optimization. Acta Mechanica 2002;153:183–206.
[8] Chen W. Experimental and numerical study on bending collapse of aluminum foam-filled hat profiles. International Journal of Solids and Structures 2001;38:7919–44.
[9] Kim A, Cheon SS, Hasan MA, Cho SS. Bending behavior of thin-walled cylindrical tube filled with aluminum alloy foam. Key Engineering Materials 2004;270-273:46–51.
[10] Hanssen AG, Hopperstad OS, Langseth M. Bending of square aluminum extrusions with aluminum foam filler. Acta Mechanica 2000;142:13–31.
[11] Reyes A, Hopperstad OS, Hanssen AG, Langseth M. Modeling of material failure in foam-based components. International Journal of Impact Engineering 2004;30:805–34.
[12] Guo, L.W., Yu, J.L., Bending behavior of aluminum foam-filled double cylindrical tubes, Experimental Mechanics, Submitted for publication.